İstanbul Med J 2024; 25(3): 207-13
DOI: 10.4274/imj.galenos.2024.75272

Morphometric Analysis of the Posterior Fossa and Cervical Spinal Canal in Type 1 Chiari Malformation and Its Effects on Syringomyelia Development

Tahsin Saygı[1], Ahmet Kayhan[2], Nail Demirel[3]

[1]Private Consultant, Department of Neurosurgery, İstanbul, Turkey
[2]University of Health Sciences Turkey, Haseki Training and Research Hospital, Clinic of Neurosurgery, İstanbul, Turkey
[3]University of Health Sciences Turkey, İstanbul Training and Research Hospital, Clinic of Neurosurgery, İstanbul, Turkey

ABSTRACT

Introduction: Chiari malformation (CIM) is a congenital anomaly characterized by herniation of hindbrain structures through the foramen magnum into the cervical spinal canal (CSC). Although the pathogenesis of CIM has not been clearly defined, its relationship with the posterior fossa and CSC morphology is unclear. In this study, we aimed to perform morphometric analysis of both the posterior fossa and the CSC in CIM to investigate the correlation of measurements with each other and to reveal their effects on the development of syringomyelia (SM), which has not been previously reported.

Methods: Magnetic resonance imaging images of 90 patients and 30 healthy individuals were retrospectively analyzed. Posterior fossa parameters and CSC diameters at all cervical vertebral levels were measured for each patient. The taper ratio of CSC was calculated separately for each group at the C1-C4 and C1-C7 levels. The average CSC shape was drawn for each group.

Results: No statistically significant difference was detected between the age groups. A steeper taper ratio was detected when CIM was accompanied by SM. In addition, the posterior fossa had a narrower volume than the normal fossa in CIM.

Conclusion: Morphometric analysis of both the posterior fossa and the CSC was performed using CIM for the first time in the literature. This is the first study to present the term "tapering" with an illustration.

Keywords: Chiari malformation, posterior fossa, syringomyelia, morphometric analysis, taper ratio

Introduction

Chiari malformation (CIM) is a congenital anomaly characterized by herniation of the hindbrain structures through the foramen magnum into the cervical spinal canal (CSC). Although there are different forms of CIM, the most common is type 1, which is characterized by displacement of the cerebellar tonsils toward the upper CSC and may be accompanied by syringomyelia (SM). Other types of CIM may also be accompanied by hydrocephalus, craniosynostosis, tethered spinal cord syndrome, and various bone abnormalities in addition to SM (1).

Although the pathogenesis of CIM has not been clearly defined, it has been hypothesized that the underdeveloped posterior fossa region creates congestion on the hindbrain, leading to herniation and SM formation, and various morphometric studies in the literature support this hypothesis (2-6). It has been reported that SM in CIM may occur as a result of abnormal cerebrospinal fluid (CSF) dynamics (7). In addition, previous studies have investigated the effect of the morphology of CSC on the development of SM in CIM (8-10). Although there are also studies in which morphometric analysis of the posterior fossa is performed in CIM (5,6,11), no study has evaluated morphometric analysis of both the posterior fossa and the CSC together. In this study, our aim was to perform morphometric analysis of both the posterior fossa and the CSC in CIM to investigate the correlation of measurements with each other and to reveal their effects on the development of SM.

Methods

Ethical Approval

This study was approved by the chairmanship of the Clinical Research Ethics Committee of the University of Health Sciences Turkey, Haseki Training and Research Hospital (approval number: 65-2023, date: 29.03.2023).

Address for Correspondence: Tahsin Saygı MD, Private Consultant, Department of Neurosurgery, İstanbul, Turkey
Phone: +90 507 788 69 36 **E-mail:** tahsinsaygi@yahoo.com **ORCID ID:** orcid.org/0000-0002-3300-1582

Cite this article as: Saygı T, Kayhan A, Demirel N. Morphometric Analysis of the Posterior Fossa and Cervical Spinal Canal in Type 1 Chiari Malformation and Its Effects on Syringomyelia Development. İstanbul Med J. 2024; 25(3): 207-13

Received: 14.01.2024
Accepted: 24.05.2024

Patients

Within the scope of this study, magnetic resonance imaging (MRI) of patients who applied to our hospital between 2014 and 2023 and were diagnosed with CIM and/or idiopathic SM were retrospectively examined. The cases were collected in 4 different groups. 30 patients with only CIM were included in Group 1, 30 patients with CIM and SM were included in Group 2, and 30 patients with idiopathic SM were included in Group 3. Thirty patients who applied to our hospital for a different reason were included in Group 4, which comprised the control group.

Inclusion and Exclusion Criteria

The inclusion criterion for patients with CIM to be included in the study was determined as cerebellar tonsillar herniation >3 millimeters (mm) and above. The inclusion criterion for idiopathic SM was determined as the presence of cervical or cervicothoracic SM without pathology causing SM, such as cerebellar tonsillar herniation, neoplasm, trauma, and infection. Cases with a history of occipitocervical surgery, craniocervical trauma, spinal dysraphism, spinal cord disease other than SM, cervical degenerative disease narrowing the spinal subarachnoid space, significant cervical flattening and/or kyphosis, hydrocephalus, and peripheral nerve entrapment neuropathy were excluded from the study.

Radiological Measurement

Radiological evaluation was performed using midsagittal T2 sequence MRI images of patients (GE Healthcare) scanned at 1.5 Tesla quality and 3 mm thickness. The degree of tonsillar herniation was calculated by considering the length (in mm) of the line drawn perpendicularly from the tip of the cerebellar tonsil to the line connecting the basion and opisthion.

For the morphometric analysis of the posterior fossa, clivus length (the line extending between the highest point of the dorsum sella and the basion), anteroposterior diameter of the foramen magnum (the line connecting the basion and the opisthion), supraocciput length (the line between the center of the internal occipital protuberance and the opisthion), posterior fossa diameter (line extending parallel to the basion-opisthion line from above the dorsum sella to the internal occipital protuberance), and posterior fossa height (line extending perpendicularly from the splenium to the basion-opisthion line) were measured separately for each patient and recorded in millimeters (Figure 1).

For the morphometric analysis of the CSC, the diameter of the spinal canal was measured at all cervical vertebral levels. To confirm the midsagittal view, we checked that the spinous processes were equally visible at all levels and that we were in the midline in the axial view. Measurements were performed by placing a line perpendicular to the spinal canal from the midpoint of the distance between the upper and lower endplates of the vertebra along the anteroposterior border of the subarachnoid space in the vertebrae, except for C2. Measurements at the C2 level were made by placing a line perpendicular to the spinal canal from the midpoint of the distance between the upper and lower endplates of the corpus along the anteroposterior border of the subarachnoid space (Figure 2). Using this method, the diameters of the spinal canal at levels C1-C7 were measured and were noted as mm in all groups. After measurement, a linear trend line was fitted by least squares regression with an algorithm resident in the Microsoft Excel spreadsheet (Microsoft, Redmond, Washington), and the slope of this line was recorded as the taper ratio (mm/level). The taper ratio was calculated separately for each group at the C1-C4 and C1-C7 levels.

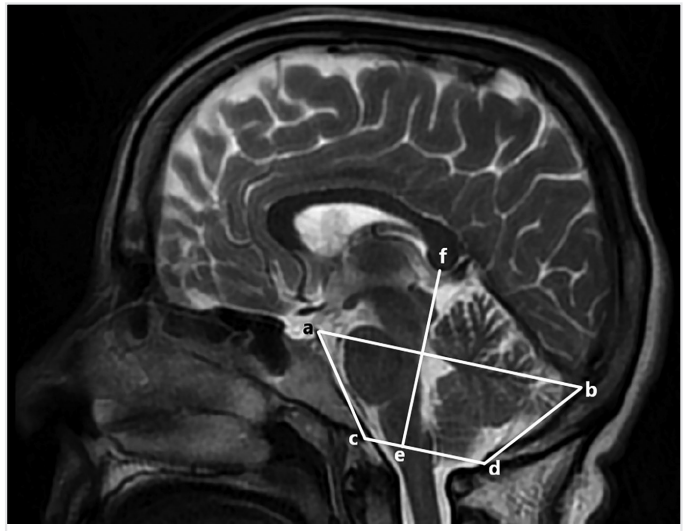

Figure 1. Posterior fossa measurement method made on mid-sagittal T2-weighted MRI of a healthy case
a: Dorsum sella, b: Center of the internal occipital protuberance, c: Basion, d: Opisthion, e: Contact point of the line perpendicular to the foramen magnum diameter, f: Inferior aspect of the splenium, a, b: Posterior fossa diameter, c, d: Foramen magnum diameter, a, c: Clivus length, b, d: Supraocciput length, e, f: Posterior fossa height
MRI: Magnetic resonance imaging

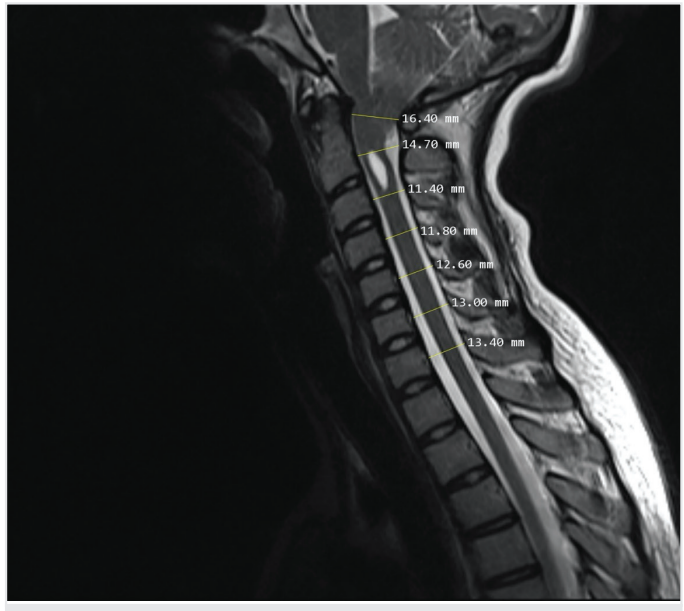

Figure 2. Cervical spinal canal measurement method using mid-sagittal T2-weighted MRI of a Group 2 case
MRI: Magnetic resonance imaging

Illustration

The average CSC shape was drawn for each group using Adobe Illustrator 2022 (Adobe Inc., California, USA) based on the average foramen magnum diameters and average CSC diameters of the groups. Average vertebral height values reported in the literature were used for figure drawing. The average height values were accepted as 5 mm for C1 (12), the sum of 15.4 (posterior height of the odontoid) and 17.9 (posterior height of the body of C2) for C2 (13), and 10 mm for typical cervical vertebrae (14). When calculating the spinal canal diameter at the C1 level, the total thickness of the odontoid process and ligaments was maintained constant at 15 mm.

Statistical Analysis

The Number Cruncher Statistical System (NCSS LLC, Kaysville, Utah, USA) 2020 statistical software for Windows was used to analyze the study data. We expressed quantitative variables as mean, standard deviation, median, minimum, and maximum values, and descriptive statistical methods, such as frequency and percentage, for qualitative variables. Shapiro-Wilks test and Box Plot graphics were used to evaluate the suitability of the data for normal distribution. Predictive values were obtained by linear regression analysis for the calculation of taper ratios. One-Way ANOVA was used to evaluate normally distributed variables according to groups, and Bonferroni's test was used for post hoc comparisons to determine the group that caused the difference. Pearson's chi-square test was used to compare qualitative data. The results were evaluated at the 95% confidence interval and the significance level was set as $p<0.05$.

Results

The descriptive statistics of patients' age and gender by group are summarized in Table 1. No statistically significant differences were detected between the groups in terms of age distribution ($p>0.05$). The gender distribution was approximately 2:1 in favor of females (Table 1).

The anteroposterior diameter of the CSC was the narrowest at C4 across all groups. The level at which the groups were closest to each other in terms of CSC diameter was noted as the C3 level. The spinal canal narrowed from C1 to C4 in all groups. The taper ratios of Group 2 were noted to be significantly steeper than other groups ($p<0.01$). The taper ratios of Groups 1 and 3 were similar to those of Group 4 ($p>0.05$) (Table 2). It was noted that although the CSC diameter of 9 patients in Group 1 was similar to the diameter measurements in Group 2, SM did not develop. The trendline graphic obtained from the CSC diameter measurements of the Groups is shown in Figure 3. The taper ratios of the groups were also presented graphically (Figure 4). As a result of the illustration of the average foramen magnum diameter and average CSC diameters of the groups, it was noted that there was a rapid narrowing in Group 2 compared with the other groups, especially at the C1-C3 levels (Figure 5).

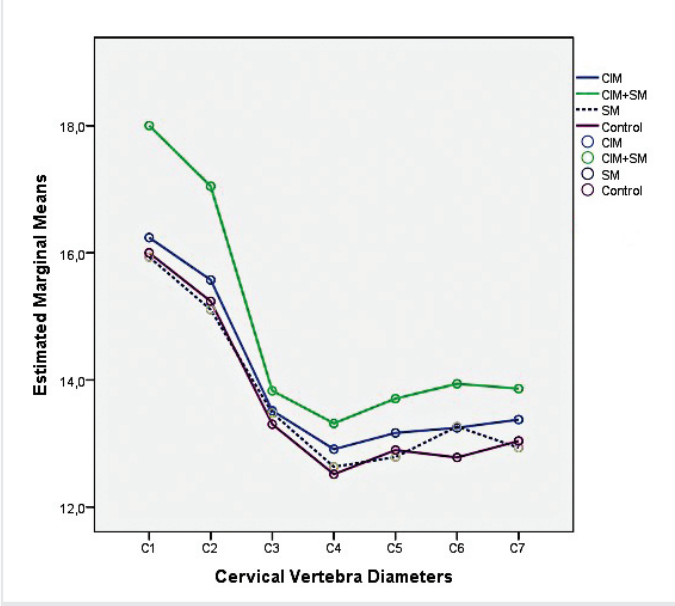

Figure 3. Trendline graph of cervical vertebral diameters according to groups
CIM: Chiari malformation, SM: Syringomyelia

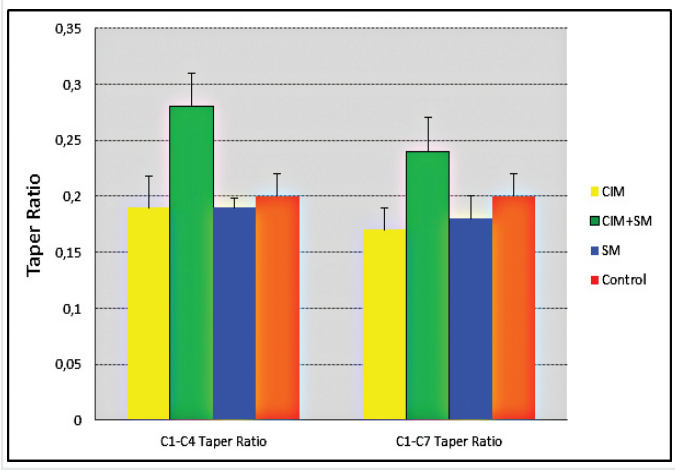

Figure 4. Distribution of C1-C4 and C1-C7 taper ratio values by groups
CIM: Chiari malformation, SM: Syringomyelia

Table 1. Descriptive statistics of patients' age and sex by group

Groups		Group 1 (CIM) (n=30)	Group 2 (CIM + SM) (n=30)	Group 3 (SM) (n=30)	Group 4 (control) (n=30)	p
Gender	Men	9 (30.0)	11 (36.7)	13 (43.3)	10 (33.3)	**0.737**[a]
	Women	21 (70.0)	19 (63.3)	17 (56.7)	20 (66.7)	-
Age	Mean ± SD	38.03±6.62	38.3±7.41	41.77±8.31	37.4±8.04	**0.172**[b]
	Median (min.-max.)	37.5 (26-50)	40 (24-51)	41.5 (27-55)	35.5 (19-49)	-

[a]Pearson's chi-square test, [b]One-Way ANOVA test, CIM: Chiari malformation, SM: Syringomyelia, SD: Standard deviation, min.: Minimum, max.: Maximum

Table 2. Descriptive statistics of cervical vertebra diameters and taper ratio

		Group 1 [A]CIM (n=30)	Group 2 [B]CIM + SM (n=30)	Group 3 [C]SM (n=30)	Group 4 [D]control (n=30)	[b]p	A-B	A-C	A-D	B-C	B-D	C-D
C1	Mean ± SD	16.24±0.79	18.00±0.88	15.93±0.75	16.00±0.59	**0.001****	**0.001**	0.729	1,000	0.001	**0.001**	1,000
	Median (min.-max.)	16 (15.2-17.4)	18.1 (16.4-19.7)	15.8 (15-17.4)	16 (15-17.5)							
C2	Mean ± SD	15.57±0.60	17.05±1.01	15.11±0.69	15.24±0.53	**0.001****	**0.001**	0.088	0.460	**0.001**	**0.001**	1,000
	Median (min.-max.)	15.4 (14.8-16.7)	17.2 (14.7-19)	15 (14.1-16.4)	15.1 (14.5-16.4)							
C3	Mean ± SD	13.52±0.62	13.83±0.80	13.48±0.63	13.30±0.44	**0.016***	0.352	1,000	1,000	0.211	**0.010**	1,000
	Median (min.-max.)	13.5 (12.4-15.2)	13.9 (11.4-15.1)	13.2 (12.4-14.7)	13.2 (12.8-14.2)							
C4	Mean ± SD	12.94±0.54	13.32±0.66	12.63±0.55	12.52±0.38	**0.001****	**0.027**	0.307	0.036	**0.001**	**0.001**	1,000
	Median (min.-max.)	12.8 (12.2-14.4)	13.5 (11.8-14.4)	12.4 (12-13.6)	12.5 (12-13.3)							
C5	Mean ± SD	13.17±0.63	13.71±0.61	12.79±0.67	12.90±0.38	**0.001****	**0.003**	0.078	0.454	**0.001**	**0.001**	1,000
	Median (min.-max.)	13 (12.4-15)	13.8 (12.6-14.6)	12.5 (12-14.1)	12.9 (12.3-13.7)							
C6	Mean ± SD	13.25±0.66	13.94±0.60	13.27±0.65	12.78±0.47	**0.001****	**0.001**	1,000	**0.019**	**0.001**	**0.001**	**0.013**
	Median (min.-max.)	13 (12-14.9)	13.9 (13-14.8)	13.1 (12.5-14.6)	12.8 (12.2-13.5)							
C7	Mean ± SD	13.38±0.68	13.86±0.63	12.93±0.62	13.04±0.40	**0.001****	**0.011**	**0.026**	0.176	**0.001**	**0.001**	1,000
	Median (min.-max.)	13.2 (12.3-15)	13.8 (12.8-15.1)	12.8 (12.2-14.3)	13 (12.3-13.8)							
C1-C4 taper ratio	Mean ± SD	0.19±0.028	0.28±0.03	0.19±0.02	0.20±0.02	[b]**0.001****	**0.001**	1,000	0.593	**0.001**	**0.001**	0.630
	Median (min.-max.)	0.20 (0.12-0.25)	0.27 (0.20-0.34)	0.19 (0.16-0.22)	0.20 (0.17-0.25)							
C1-C7 taper ratio	Mean ± SD	0.17±0.02	0.24±0.03	0.18±0.02	0.17±0.02	[b]**0.001****	**0.001**	1,000	1,000	**0.001**	**0.001**	1,000
	Median (min.-max.)	0.17 (0.14-0.21)	0.24 (0.18-0.32)	0.17 (0.13-0.22)	0.18 (0.14-0.23)							

[b]One-way ANOVA & post-hoc Bonferroni test, *p<0.05, **p<0.01. CIM: Chiari malformation, SM: Syringomyelia, SD: Standard deviation

When the posterior fossa measurement results of the groups were compared, it was calculated that the height, posterior fossa diameter, supraocciput, and clivus length were statistically smaller in Groups 1 and 2 than in Groups 3 and 4 (p<0.01). In contrast, the foramen magnum diameter length was statistically larger in Groups 1 and 2 than in Groups 3 and 4 (p<0.01). Comparing all Groups, Group 2 had the narrowest posterior fossa, and Group 1 had the narrowest posterior fossa (Table 3).

Discussion

Despite its long history, the pathophysiology of CIM is still not clearly understood, and its treatment remains controversial (15). The opinions are contradictory, especially regarding patients who are asymptomatic or have a mild clinical course. The presence of SM in these patients affects the surgical decision (16). However, there are also case reports in the literature stating that SM and tonsillar herniation can be spontaneously resolved in CIM (17-21). There are many hypotheses regarding the pathophysiology of SM, but the most accepted one is that CSF enters the central canal with arterial pulsation but cannot return because the narrowed part of the central canal acts as a one-way valve (22).

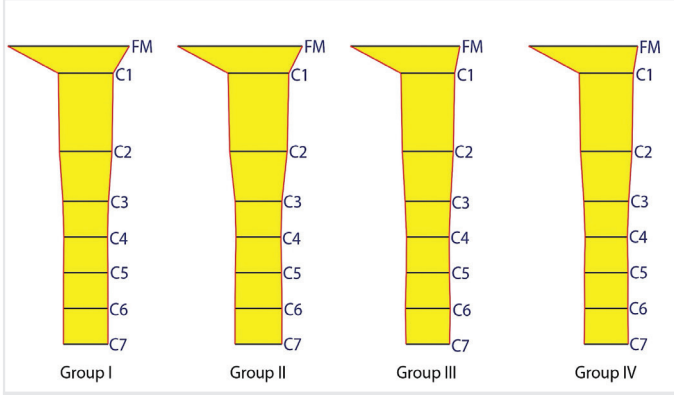

Figure 5. Illustration showing the average foramen magnum diameter and average cervical spinal canal diameters of the groups

Conversely, no relationship could be established between the degree of herniation in CIM and the severity of complaints (6,23).

Research is ongoing to resolve the debates regarding both etiopathogenesis and treatment strategies in CIM. Some of these analyses are morphometric analyses performed on radiological data.

Table 3. Descriptive statistics of the posterior fossa measurements

		Group 1 [A]CIM (n=30)	Group 2 [B]CIM + SM (n=30)	Group 3 [C]SM (n=30)	Group 4 [D]control (n=30)	Toplam	[b]p	A-B	A-C	A-D	B-C	B-D	C-D
Height	Mean ± SD	54.62±3.81	53.36±3.05	62.44±5.54	61.92±3.79	58.09±5.82	**0.001****	1,000	**0.001**	**0.001**	**0.001**	**0.001**	1,000
	Median (min.-max.)	53.5 (49.5-61.7)	53.2 (48.9-58.9)	60 (54.3-71.1)	61.3 (55.5-68)	57.7 (48.9-71.1)							
Foramen magnum	Mean ± SD	36.05±2.49	37.04±2.20	32.49±2.18	32.35±1.54	34.48±2.97	**0.001****	0.460	**0.001**	**0.001**	**0.001**	**0.001**	1,000
	Median (min.-max.)	36.3 (31.6-40.1)	37 (33.5-40.8)	32.4 (29.1-36.3)	32.3 (29.8-36.4)	34.1 (29.1-40.8)							
Posterior fossa diameter	Mean ± SD	75.49±4.24	74.18±4.42	85.41±6.34	86.96±1.80	80.51±7.26	**0.001****	1,000	**0.001**	**0.001**	**0.001**	**0.001**	1,000
	Median (min.-max.)	76.8 (68.3-81)	74.8 (65.1-82.8)	85.3 (71.6-94.1)	86.6 (84.3-90.2)	80.6 (65.1-94.1)							
Supraocciput	Mean ± SD	42.11±4.88	41.09±2.76	50.85±2.79	49.68±2.41	45.93±5.49	**0.001****	1,000	**0.001**	**0.001**	**0.001**	**0.001**	1,000
	Median (min.-max.)	41.8 (34.7-49.9)	41.2 (37.1-46.4)	50.4 (47.1-56.1)	49.1 (45.5-54)	47.1 (34.7-56.1)							
Clivus	Mean ± SD	39.61±5.08	36.34±6.32	44.94±2.77	46.25±2.85	41.78±6	**0.001****	**0.036**	**0.001**	**0.001**	**0.001**	**0.001**	1,000
	Median (min.-max.)	39.6 (32.6-46.8)	33.7 (28.1-44.7)	44.4 (40.1-49.4)	45.5 (41.5-51.3)	43.4 (28.1-51.3)							

[b]One-Way ANOVA and Bonferroni tests, **p<0.01, CIM: Chiari malformation, SM: Syringomyelia, SD: Standard deviation

While some authors focused on the morphometric analysis of the posterior fossa, others focused on the morphometric analysis of the CSC. As a result of the measurements, the authors generally stated that there was a decrease in the measurement values of the posterior fossa compared with normal and that this situation leads to congestion in the posterior fossa, causing herniation (5,6,24-26). Basaran et al. (27) drew attention to another point in their morphometric analysis of CIM. They reported that the posterior fossa volume was normal in CIM, but because the total intracranial volume increased compared with normal, the pathophysiology was processed due to a proportional decrease in the posterior fossa volume.

Studies on the morphometric analysis of the CSC in CIM are generally concerned with the extent to which the diameter of the spinal canal narrows. The results of the studies conducted on this subject do not agree with each other. Thompson et al. (28) compared the C1-4, C4-7, and C1-7 taper ratios of CIM + SM with those of CIM and found that the CIM + SM group had a steeper taper ratio in the C4-7. According to this result, the authors hypothesized that the morphology of the lower cervical region may lead to the development of SM. Hirano et al. (8) compared the C1-7 taper ratio between CIM + SM, CIM, SM, and healthy individuals. In the analysis, it was determined that there was a steeper taper ratio in the upper CSC in CIM + SM than in other regions, and it was noted that there was a mesodermal anomaly in CIM (8). Gadde et al. (10) investigated the role of the taper ratio in the transformation of presyrinx to SM in CIM and found that the taper ratios at C1-4 and C1-7 were steeper in patients with presyrinx. Zhu et al. (9) drew attention to a different point and compared the taper ratio in distended SM with that in non-distended SM and stated that, contrary to other studies, the taper ratio was steeper in the non-distended group. Hammersley et al. (29) drew attention to yet another point and compared CIM patients with and without scoliosis; in their analysis, they stated that there was a steeper taper ratio in those with scoliosis and CIM. Thakar et al. (30) analyzed both the taper ratio and the changes in the paraspinal muscles in CIM. They stated, similar to the literature, that there is a steeper tapering in CIM; there is also atrophy in the paraspinal muscles, and this atrophy may be related to the steeper tapering (30).

The results of all these studies suggest that the morphology of CIM is different from normal. Although there have been many morphometric analyses in CIM of the posterior fossa and the CSC, no study has been conducted regarding both the posterior fossa and the CSC morphometry in the literature. In this study, unlike previous studies, measurements were made for both regions, and the results were evaluated together. According to our findings, posterior fossa dimensions are generally reduced in CIM with or without SM. It is also understood that when SM is accompanied by CIM, the posterior fossa dimensions become narrower. Our findings regarding spinal canal morphometry indicate a relationship between SM accompanying CIM and steeper tapering. Although there are many studies on spinal canal tapering in CIM, this study presents the term "tapering" with an illustration for the first time in the literature. The aim of this study was to better understand the effect of tapering on the development of SM. However, it was observed that the CSC diameters of 9 patients in Group 1 were similar to those of the patients in Group 2. Nevertheless, SM did not develop in these

patients. Based on these findings, CSC morphology alone may not be sufficient for the development of SM. In this regard, a prospective study with long-term follow-up of patients with tapering rates similar to those in Group 2 may help early detect patients with CIM who are likely to develop SM in the future. We believe that studies with a larger patient population are necessary.

Study Limitations

This retrospective study was based on radiological data. Further prospective studies with a larger patient group, including clinical information and long-term follow-up.

Conclusion

In this study, for the first time in the literature, morphometric analysis of both the posterior fossa and the CSC was performed using CIM. Consistent with the literature, our results showed that both the posterior fossa and CSC morphometry were different between CIM and normal subjects. In addition, although there are many studies on the CSC taper ratio, this is the first study to present the term "tapering" with an illustration. We believe that our results will help reduce the debate about the etiology and treatment of CIM.

Ethics Committee Approval: This study was approved by the chairmanship of the Clinical Research Ethics Committee of the University of Health Sciences Turkey, Haseki Training and Research Hospital (approval number: 65-2023, date: 29.03.2023).

Informed Consent: Retrospective study.

Authorship Contributions: Concept - T.S.; Design - T.S.; Data Collection or Processing - T.S., A.K.; Analysis or Interpretation - T.S., A.K., N.D.; Literature Search - T.S., A.K., N.D.; Writing - T.S., A.K., N.D.

Conflict of Interest: No conflict of interest was declared by the authors.

Financial Disclosure: The authors declared that this study received no financial support.

References

1. George TM, Higginbotham NH. Defining the signs and symptoms of Chiari malformation type I with and without syringomyelia. Neurol Res. 2011; 33: 240-6.
2. Milhorat TH, Nishikawa M, Kula RW, Dlugacz YD. Mechanisms of cerebellar tonsil herniation in patients with Chiari malformations as guide to clinical management. Acta Neurochir (Wien). 2010; 152: 1117-27.
3. Sgouros S, Kountouri M, Natarajan K. Posterior fossa volume in children with Chiari malformation Type I. J Neurosurg. 2006; 105: 101-6.
4. Tubbs RS, Hill M, Loukas M, Shoja MM, Oakes WJ. Volumetric analysis of the posterior cranial fossa in a family with four generations of the Chiari malformation Type I. J Neurosurg Pediatr. 2008; 1: 21-4.
5. Nishikawa M, Sakamoto H, Hakuba A, Nakanishi N, Inoue Y. Pathogenesis of Chiari malformation: a morphometric study of the posterior cranial fossa. J Neurosurg. 1997; 86: 40-7.
6. Aydin S, Hanimoglu H, Tanriverdi T, Yentur E, Kaynar MY. Chiari type I malformations in adults: a morphometric analysis of the posterior cranial fossa. Surg Neurol. 2005; 64: 237-41.
7. Pinna G, Alessandrini F, Alfieri A, Rossi M, Bricolo A. Cerebrospinal fluid flow dynamics study in Chiari I malformation: implications for syrinx formation. Neurosurg Focus. 2000; 8: E3.
8. Hirano M, Haughton V, Munoz del Rio A. Tapering of the cervical spinal canal in patients with Chiari I malformations. AJNR Am J Neuroradiol. 2012; 33:1326-30.
9. Zhu Z, Sha S, Sun X, Liu Z, Yan H, Zhu W, et al. Tapering of the cervical spinal canal in patients with distended or nondistended syringes secondary to Chiari type I malformation. AJNR Am J Neuroradiol. 2014; 35: 2021-6.
10. Gadde JA, Shah V, Liebo GB, Ringstad GA, Pomeraniec IJ, Bakke SJ, et al. Anatomical features of the cervical spinal canal in Chiari I deformity with presyrinx: A case-control study. Neuroradiol J. 2017; 30: 405-9.
11. Noudel R, Jovenin N, Eap C, Scherpereel B, Pierot L, Rousseaux P. Incidence of basioccipital hypoplasia in Chiari malformation type I: comparative morphometric study of the posterior cranial fossa. Clinical article. J Neurosurg. 2009; 111: 1046-52.
12. Gosavi SN, Vatsalaswamy P. Morphometric Study of the Atlas Vertebra using Manual Method. Malays Orthop J. 2012; 6: 18-20.
13. Naderi S, Arman C, Güvençer M, Korman E, Senoglu M, Tetik S, et al. Morphometric analysis of the C2 body and the odontoid process. Turkish Neurosurgery. 2006; 16: 14-8.
14. Prameela MD, Prabhu LV, Murlimanju BV, Pai MM, Rai R, Kumar CG. Anatomical dimensions of the typical cervical vertebrae and their clinical implications. Eur J Anat. 2020; 24: 9-15.
15. Frič R, Eide PK. Chiari type 1-a malformation or a syndrome? A critical review. Acta Neurochir (Wien). 2020; 162: 1513-25.
16. Massimi L, Peretta P, Erbetta A, Solari A, Farinotti M, Ciaramitaro P, et al. Diagnosis and treatment of Chiari malformation type 1 in children: the International Consensus Document. Neurol Sci. 2022; 43: 1311-26.
17. Cuthbert H, Pepper J, Price R. Spontaneous resolution of a Chiari malformation with syringomyelia. BMJ Case Rep. 2021; 14: e241789.
18. Gallo E, Rahmathulla G, Rao D, Tavanaiepour K, Tavanaiepour D. Spontaneous syrinx resolution in patient with Chiari I malformation: illustrative case. J Neurosurg Case Lessons. 2021; 1: CASE21236.
19. Sun PP, Harrop J, Sutton LN, Younkin D. Complete spontaneous resolution of childhood Chiari I malformation and associated syringomyelia. Pediatrics. 2001; 107: 182-4.
20. Avellino AM, Britz GW, McDowell JR, Shaw DW, Ellenbogen RG, Roberts TS. Spontaneous resolution of a cervicothoracic syrinx in a child. Case report and review of the literature. Pediatr Neurosurg. 1999; 30: 43-6.
21. Strahle J, Muraszko KM, Kapurch J, Bapuraj JR, Garton HJ, Maher CO. Natural history of Chiari malformation Type I following decision for conservative treatment. J Neurosurg Pediatr. 2011; 8: 214-21.
22. Koyanagi I, Houkin K. Pathogenesis of syringomyelia associated with Chiari type 1 malformation: review of evidences and proposal of a new hypothesis. Neurosurg Rev. 2010; 33: 271-84.
23. Aboulezz AO, Sartor K, Geyer CA, Gado MH. Position of cerebellar tonsils in the normal population and in patients with Chiari malformation: a quantitative approach with MR imaging. J Comput Assist Tomogr. 1985; 9: 1033-6.
24. Vurallı D, Oksüzler M. Radiological determination of fossa cranii posterior morphometry in Chiari malformation type I. Cukurova Medical Journal. 2022; 47: 1067-72.
25. Dagtekin A, Avci E, Kara E, Uzmansel D, Dagtekin O, Koseoglu A, et al. Posterior cranial fossa morphometry in symptomatic adult Chiari I malformation patients: comparative clinical and anatomical study. Clin Neurol Neurosurg. 2011; 113: 399-403.

26. Yan H, Han X, Jin M, Liu Z, Xie D, Sha S, et al. Morphometric features of posterior cranial fossa are different between Chiari I malformation with and without syringomyelia. Eur Spine J. 2016; 25: 2202-9.

27. Basaran R, Efendioglu M, Senol M, Ozdogan S, Isik N. Morphometric analysis of posterior fossa and craniovertebral junction in subtypes of Chiari malformation. Clin Neurol Neurosurg. 2018; 169: 1-11.

28. Thompson A, Madan N, Hesselink JR, Weinstein G, Munoz del Rio A, Haughton V. The Cervical Spinal Canal Tapers Differently in Patients with Chiari I with and without Syringomyelia. AJNR Am J Neuroradiol. 2016; 37: 755-8.

29. Hammersley J, Haughton V, Wang Y, del Rio AM. Tapering of the cervical spinal canal in patients with scoliosis with and without the Chiari I malformation. AJNR Am J Neuroradiol. 2012; 33: 1752-5.

30. Thakar S, Kurudi Siddappa A, Aryan S, Mohan D, Sai Kiran NA, Hegde AS. Does the mesodermal derangement in Chiari Type I malformation extend to the cervical spine? Evidence from an analytical morphometric study on cervical paraspinal muscles. J Neurosurg Spine. 2017; 27: 421-7.